Available online at www.sciencedirect.com
ScienceDirect
Journal of Magnetic Resonance 185 (2007) 12–18
JMR Journal of Magnetic Resonance
www.elsevier.com/locate/jmr

Locating hydrogen atoms in single crystal and uniaxially aligned amino acids by solid-state NMR

Benjamin J. Gross, Ann E. McDermott *

Department of Chemistry, Columbia University, New York, NY 10027, USA

Received 9 June 2006; revised 23 September 2006
Available online 4 December 2006

Abstract

We demonstrate a novel method to locate hydrogen atoms in amino acids, which involves measuring the $C_\alpha H_\alpha$ bond vector geometry through orientationally dependent dipolar coupling frequencies measured by Lee–Goldburg cross polarization (LGCP). A 2D LGCP experiment is used to measure the polar angle of the $C_\alpha H_\alpha$ bond vector in a single crystal of the model compound L-alanine. It is also demonstrated that by coupling the $^{13}C_\alpha{}^{1}H_\alpha$ LGCP experiment to a $^{13}C_\alpha{}^{15}N$ REDOR experiment, one can determine the complete three-dimensional geometry of the $C_\alpha H_\alpha$ and $C_\alpha N$ vectors in a single crystal. These measurements allow for location of hydrogen atoms in crystalline biological macromolecules.

Keywords: Magic angle oriented sample spinning (MAOSS); Single crystal NMR; LGCP; REDOR; Solid-state NMR; Structure determination; Biopolymers; Dipolar coupling

1. Introduction

Solid-state nuclear magnetic resonance (SSNMR) is a new method for solving protein structures, with the potential to be a powerful approach to studying certain classes of membrane proteins and large (>25 kDa) biological macromolecular systems. Spectral resolution for complex systems has been ever improving, due to creative labeling schemes, advanced pulse sequences, and a new generation of high-field magnets, thus making SSNMR an increasingly attractive experimental method for the structural biology community. In the recent past a small number of protein structures have been solved [2–4] and deposited in the Protein Data Bank [5,6], based on SSNMR methods.

This report focuses on the specific problem of locating hydrogen atoms through orientational constraints, in the context of structure determination by high resolution SSNMR. The use of angular or orientational constraints, determined for a samples oriented with respect to an external frame of reference, can facilitate dramatically improved structure calculations, as compared with those based solely on distance constraints, and has a significant precedent in existing solution and static solid-state protein NMR literature [7–9]. The study of hydrogen, rather than heavier atoms, illustrates a well-known opportunity for NMR relative to diffraction methods as it is not generally possible to locate hydrogen atoms with moderate resolution X-ray diffraction data; and although neutron diffraction is a good technique for this purpose, the experimental demands are considerable. In addition, while X-ray crystallography has contributed tremendously to our understanding of cellular processes and molecular specificity, and is the benchmark in protein structure determination, its range of applicability suffers from the need for single crystals, which can present a formidable challenge in many cases [1]. As an alternative, SSNMR has the capacity to locate (in three dimensions) hydrogen atoms in biological solids by measuring the geometrically dependent heteronuclear dipolar coupling values (ω_D) between ^{1}H nuclei and their neighboring nuclei (typically ^{13}C or ^{15}N), as illustrated in this report.

* Corresponding author. Fax: +1 212 932 1289.
E-mail addresses: bjg30@columbia.edu (B.J. Gross), aem5@columbia.edu (A.E. McDermott).

1090-7807/$ - see front matter © 2007 Published by Elsevier Inc.
doi:10.1016/j.jmr.2006.09.025

A number of high resolution magic angle spinning (MAS) SSNMR techniques exist that measure heteronuclear couplings in isotropic samples for the purpose of internuclear distance determination. Some of these methods, when applied to aligned samples, can provide orientational information based on the dipolar tensor. Studies by high resolution MAS SSNMR, probing the orientation of vectors in a molecular frame using a sample uniaxially oriented with respect to the MAS rotor axis, have also been reported, although there are relatively few examples to date [10,11]. MAS SSNMR methods for probing ^{1}H–^{13}C couplings are herein used for the first time to provide angular constraints for a CH bond vector. In order to measure ^{1}H-X heteronuclear couplings in the solid state, ^{1}H homonuclear decoupling is essential to reduce effects that serve to convolute heteronuclear dipolar spectra. To this end the Lee–Goldburg cross polarization (LGCP) experiment can be used to determine heteronuclear bond geometry while providing effective ^{1}H homonuclear decoupling [12]. LGCP is a proven method for measuring internuclear distances in isotropic solid samples between abundant large-γ spins (e.g. ^{1}H) that are strongly coupled to a dilute spin (e.g. ^{13}C, ^{15}N). LGCP is shown herein to be similarly useful for measuring the polar angle of an internuclear vector (θ_{ij}^{RFF}) in the frame of reference defined by the MAS sample rotor axis (i.e. rotor fixed frame—RFF), in samples aligned relative to the rotor. The sequence need not be rotor synchronized, and the experimental results are not dependent on the azimuthal orientation (ϕ_{ij}^{RFF}) of the internuclear vector. Additionally the full three-dimensional geometry of the $C_\alpha H_\alpha$ vectors can be determined in relation to the neighboring $C_\alpha N$ bond vector orientation which can be completely determined by rotational echo double resonance (REDOR) when the sample is completely oriented with respect to the rotor axis (i.e. a single crystal).

We address the particular challenge presented by molecules packed in an environment where several asymmetric units with identical chemical shifts are disposed differently in the unit cell. To this end, a crystalline sample of (U–^{13}C, ^{15}N) enriched L-alanine, exhibiting $P_{2_12_12_1}$ symmetry, and thus having four orientational moieties, was studied, both as a uniaxially aligned sample, and as a single crystal. The issue of resolving the angular information for the four asymmetric units (with identical chemical shifts) was addressed by combining two independent dipolar measurements in a multidimensional experiment. LGCP experiments provided angular constraints (θ_{CH}^{RFF} values) for the $C_\alpha H$ vectors in each distinct asymmetric unit, while $^{13}C_\alpha$–^{15}N REDOR experiments provided complete orientation of the $C_\alpha N$ bonds (θ_{CN}^{CFF},ϕ_{CN}^{CFF}) in each unit as well as the crystal orientation relative to the rotor axis. For the single crystal system the 3D LGCP–REDOR experiments demonstrated in this work serves to correlate the $^{13}C_\alpha$–$^{1}H_\alpha$ and $^{13}C_\alpha$–^{15}N coupling values for each asymmetric unit thus defining the three dimensional orientation of the $C_\alpha H_\alpha$ vectors by association with the $C_\alpha N$ moieties, and distinguishes all four orientations in the single crystal. This approach is expected to be of use for other more complex biological macromolecules not amenable to diffraction methods.

2. Experimental

A mixture of 10% (U–^{13}C, ^{15}N) L-alanine diluted with 90% natural abundance L-alanine was recrystallized from deionized water as described previously [13]. A single crystal, as well as a powder sample, of this mixture was used throughout this study. The single crystal (shown schematically in Fig. 1a) was immobilized in the MAS sample rotor using poly-dimethyl-siloxane (PDMS) from Dow Corning (Sylgar 184 Elastomer Kit), and the crystal orientation was verified by X-ray indexing, as described in the same prior publication.

All NMR experiments were performed on a Varian 400 Infinity Plus spectrometer using a T3 4 mm MAS probe, in a $^{1}H/^{13}C/^{15}N$ triple resonance configuration with frequencies of 396.7747, 99.7815, and 40.2065 MHz, respectively. The pulse sequence for LGCP is given in Fig. 2a. The powder and single crystal 2D LGCP experiments were

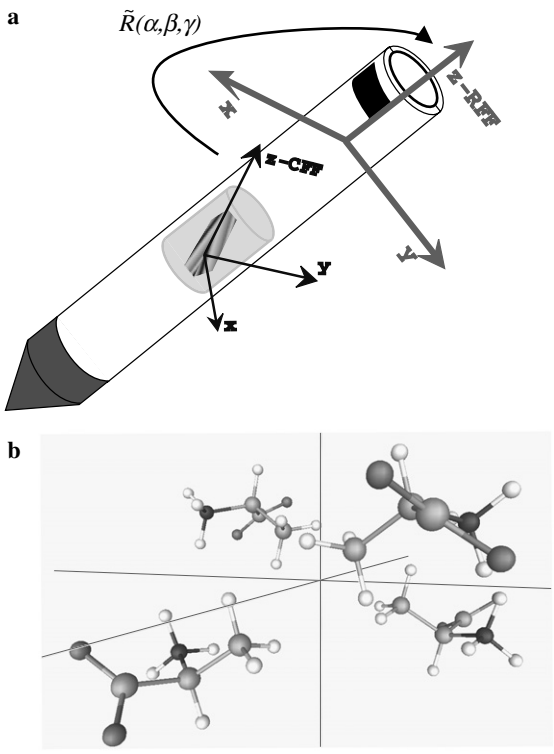

Fig. 1. (a) The spatial frame transformation from the crystal fixed frame (CFF) defined by the crystallographic axes, and the rotor fixed from (RFF) defined by the axis of sample rotation, is depicted here in this representation of the PDMS encased single crystal L-alanine sample in a MAS sample rotor. (b) The unit cell of L-alanine exhibits $P_{2_12_12_1}$ symmetry containing four distinct orientations per cell, each of which are measurable by SSNMR and indistinguishable based on isotropic chemical shifts, but must be distinguished in these studies of orientational constraints. The four orientations of the unit cell are related to one another by a 180° rotation about the crystallographic axis that separates each species in the *x*-*y* plane. This transformation is described by Eq. (6) of Section 3.

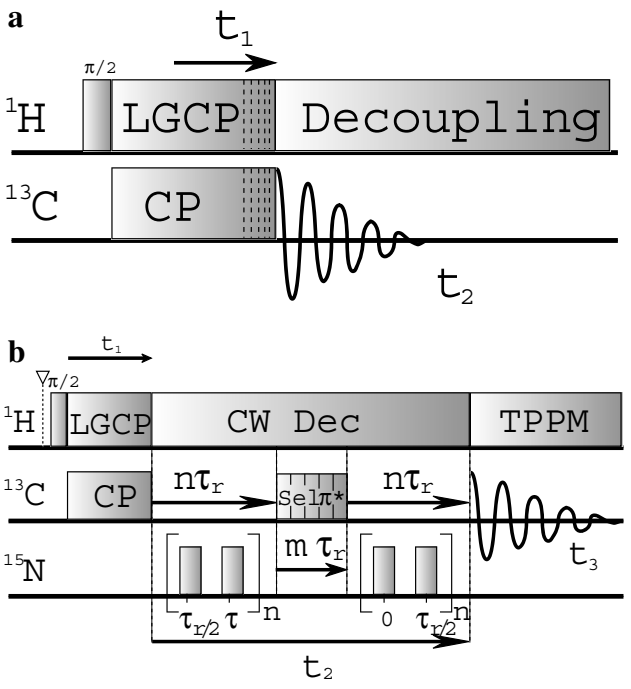

Fig. 2. (a) The 2D LGCP pulse sequence incrementally lengthens the cross polarization contact time (t_1), under Lee–Goldburg decoupling. The signal is detected during MAS so that the ^{13}C channel records a ^{13}C chemical shift spectrum, with peaks that oscillate proportional to the dipolar coupling ω_d in the indirect dimension. (b) The 3D LGCP–REDOR pulse sequence combines the LGCP evolution (t_1) for measuring ^{13}C ^{1}H couplings, with the azimuthally synchronized REDOR experiment for measuring $^{13}C^{15}N$ couplings. The timing trigger (∇) is followed by an adjustable delay to select a starting azimuthal orientation ($\gamma°$) of the spinning sample, prior to the initial π/2 pulse. The experiment identifies which bonds share the same carbon species, thus identifying the appropriate unit cell symmetry operator defining the $^{13}C_\alpha{}^{1}H_\alpha$ coupling value.

performed at a spinning speed of 14 kHz (±5 Hz) and a Lee–Goldburg decoupling field strength ($\omega^I_{\rm eff}$) of 63 kHz on the ^{1}H channel during cross polarization, with the ^{13}C channel matched to the (−1) Hartman–Hahn side band condition. The LGCP contact time of the 2D LGCP experiment was increased in increments of 20 μs to a final duration of 2.56 and 3.84 ms for the powder and single crystal, respectively. Two pulse phase modulation decoupling [14] was employed during detection.

The 2D REDOR experiments performed were based on the *J*-decoupled REDOR experiment designed for uniformly ^{13}C labeled systems [15]. The Gaussian refocusing pulse used in that work was replaced, in our experiments, by a DANTE sequence [16] due to equipment constraints. A timing trigger signal from the sample spinning speed controller maintained a constant initial azimuthal orientation between experiments, identified by the sample rotor's tachometer mark. The sample spinning frequency was maintained at 10 kHz (±5 Hz), resulting in a rotor period of 100 μs. The REDOR evolution progressed in increments of four rotor periods per data point to a total acquisition length of 38 ms. The ^{15}N REDOR π pulses were applied for a duration of 19.5 μs at half rotor intervals to generate the dipolar reduced signal (S_r). The REDOR chemical shift refocusing pulse was replaced with a DANTE pulse train, which consisted of 20 pulses of 0.5 μs duration separated by a 211 μs delay for appropriate selection of the $^{13}C_\alpha$ chemical shift. In order to occupy an integer number of rotor periods, delays of appropriate, minimal length were added before and after the DANTE sequence, the totality of which occupied approximately 4.8 ms.

The three-dimensional REDOR–LGCP experiment, the pulse sequence for which is given in Fig. 2b, was performed on the single crystal L-alanine sample encased in PDMS spinning at 10 kHz (±5 Hz). A Lee–Goldburg decoupling field strength (ω^I_{eff}) of 61 kHz on the ^{1}H channel was applied during cross polarization with the ^{13}C channel matched to the ($n = -1$) Hartman–Hahn side band condition. The LGCP contact time was increased in 60 increments, with a dwell time of 35 μs, for a final duration of 2.1 ms. The REDOR chemical shift refocusing pulse was a DANTE series (4.8 ms long), selective of the C_α resonance, while the dipolar refocusing π pulses on the ^{15}N channel were 10.2 μs in length. The REDOR duration was increased in steps of 600 μs ($6{\cdot}\tau_r$) 42 times to give a total duration of 36 ms.

Data analysis and curve fitting were performed using GNU Octave (2.1.53-1) with the GNU Octave-Forge (2004.02.12-3) functions pack on an Apple G4 Powerbook running Mac OS X (10.3) [17].

3. Results and discussion

3.1. Powder sample measurements: internuclear distance determination

A Fourier transform of the indirect dimension of the 2D LGCP experiment performed on the L-alanine powder sample yielded the dipolar spectrum in Fig. 3a, which displays the $^{13}C^{1}H$ dipolar coupling values associated with the C_α resonance. Because Lee–Goldburg decoupling was employed, the proton homonuclear coupling was ignored, and the dipolar spectrum was treated as being due to an isolated two spin system. Thus, the features of the dipolar spectrum (δ) are defined solely by the dipolar coupling constant (D, defined below) and the polar angle of the $C_\alpha H_\alpha$ internuclear vectors in the axis system of the sample rotor ($\theta^{\rm RFF}_{\rm CH}$).

$$\delta = \tfrac{3}{4} D \sin(2\theta_{\rm m}) \sin(2\theta^{\rm RFF}_{\rm CH}) \sin(\theta_{\rm m}) \quad (1)$$

where $\theta_{\rm m} = \tan^{-1}(\sqrt{2})$ is the magic angle, and

$$D = -\frac{\mu_0}{4\pi} \frac{\gamma_{\rm C}\gamma_{\rm H}\hbar}{2\pi r^3_{\rm CH}} \quad (2)$$

where γ_I is the gyromagnetic ratio for nucleus I, and $r_{\rm CH}$ is the internuclear distance.

The spectrum in Fig. 3a exhibits line shapes indicative of an isotropic powder sample (i.e. with all orientations present). Therefore in order to interpret these peaks it is not

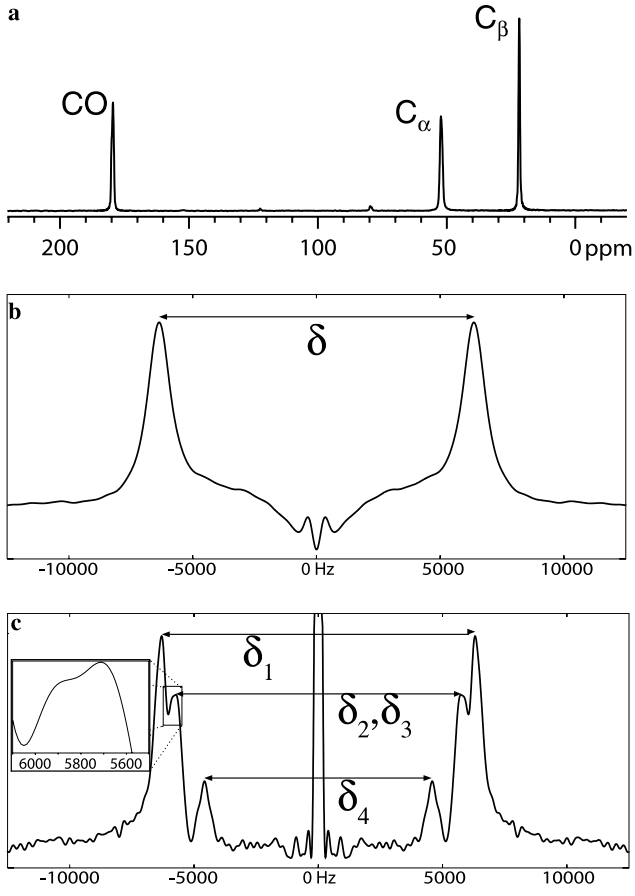

Fig. 3. (a) The $^{13}C^{1}H$ dipolar coupling spectrum of the alpha carbon collected by LGCP of the powdered L-alanine sample referenced to DSS. (b) The $^{13}C^{1}H$ dipolar coupling spectrum of the alpha carbon collected under LGCP of the powdered L-alanine sample. The peak separation (δ) is used to calculate the internuclear distance. (c) The $^{13}C^{1}H$ dipolar coupling spectrum of the alpha carbon collected under LGCP of the single crystal L-alanine sample. The peak separations (δ_k) are used to calculate the polar tilt angle of the internuclear bond vectors, with the middle two overlapping peaks enlarged in the inset to show their visible separation.

necessary to integrate $\theta_{ij}^{\mathrm{RFF}}$ over a powder distribution as the maximum peak intensity coincides with the maximum value of δ, which can be assumed to have an orientational scaling value of 1. Some considerations regarding the error in this estimate are discussed below. Thus the separation between the peak intensity maxima can be defined as

$$\delta = \tfrac{3}{4} D \sin(2\theta_{\mathrm{m}}) \sin(\theta_{\mathrm{m}}) \tag{3}$$

which can be rewritten

$$r_{\mathrm{CH}} = \frac{a}{\delta^{1/3}} \tag{4}$$

when $\theta_{ij}^{\mathrm{RFF}} = \theta_{\mathrm{CH}}^{\mathrm{RFF}} = \theta_{\mathrm{m}}$. In the case of ^{13}C and ^{1}H nuclei, $a = 25.93$ Å $\mathrm{Hz}^{1/3}$. In Ref. [10], this constant was found to be $a = 25.86$ Å $\mathrm{Hz}^{1/3}$ when extracted from measurements generated by a simulation of a two spin system. This difference of 0.3% is small, but measurable. The splitting value of the data shown in Fig. 3a is 12,683 Hz (±200 Hz), giving a distance measurement of 1.11 Å. The accuracy of the distance measurement is ultimately determined not only by the peak widths, but in a practical sense, also by the noise in the dipolar spectrum, to be approximately ±0.01 Å. This determination is in very good agreement with the X-ray estimated value of 1.13 Å [18] and more importantly with the neutron diffraction value of 1.09 Å [19]. The distance measured by dipolar coupling is expected to be slightly longer then that measured by diffraction methods [20,21], as is true for the comparison with the neutron diffraction result.

3.2. Single crystal measurements: orientation constraints

When the 2D LGCP experiment was performed on a single crystal sample of L-alanine, the dipolar spectrum exhibited four peaks (2 peaks are nearly indistinguishable) due to the aforementioned moieties of the L-alanine $P_{2_12_12_1}$ unit cell pictured in Fig. 1a. This spectral data is shown in Fig. 3b. Had any of the unit cell axes been aligned with the axis of the sample rotor, all four orientations would have shared the same dipolar coupling value, and so the L-alanine crystal used herein was intentionally tilted at a fixed angle relative to the rotor axis (as verified by X-ray measurement). Since the crystal is tilted it was possible to demonstrate the capability to measure multiple orientations simultaneously, and to provide added relevant data since up to four distinct coupling values (δ_k—also measured as peak splittings) were expected. Fitting the δ_k values shown in Fig. 3b to Eq. (1), and inserting the r_{CH} value calculated from the powder measurements, yielded the internuclear orientation vectors in Table 1, which were compared to estimates based on the crystal orientation determined by X-ray indexing, and literature crystal structures. The LGCP data interpretation is in good agreement with the crystal structure in this sense, and are estimated to be accurate to ±1°, based on the baseline RMS noise. Two of the orientations have very similar dipolar coupling values, and therefore the corresponding peaks overlap in the dipolar spectrum. The overlapping peaks correspond to two $\theta_{\mathrm{CH}}^{\mathrm{RFF}}$ values which are predicted to differ by <2.5°. There is, however partial resolution in

Table 1
Bond angular measurements relative to the rotor frame based on these oriented SSNMR experiments

	Neutron	X-ray	LGCP	REDOR
$\theta_{\mathrm{CH}\_1}^{\mathrm{RFF}}$	119.1°	119.2°	119.5°	—
$\theta_{\mathrm{CH}\_2}^{\mathrm{RFF}}$	50.2°	50.1°	53.9°	—
$\theta_{\mathrm{CH}\_3}^{\mathrm{RFF}}$	67.9°	68.1°	68.2°	—
$\theta_{\mathrm{CH}\_4}^{\mathrm{RFF}}$	122.1°	121.7°	119.5°	—
$\theta_{\mathrm{CN}}^{\mathrm{CFF}}$, $\phi_{\mathrm{CN}}^{\mathrm{CFF}}$	48.8°,165.1°	48.7°,165.0°	—	48.8°,164.6°
$\theta_{\mathrm{CH}}^{\mathrm{CFF}}$, $\phi_{\mathrm{CH}}^{\mathrm{CFF}}$	95.4°,104.0°	95.4°,103.1°	93.9°,101.8°	—

These are compared with the corresponding values from X-ray and neutron diffraction of the L-alanine alpha carbon (interpreted with knowledge of the crystal orientation). All values listed by bond type and frame of reference.

these peaks as seen in the enlarged region of interest in Fig. 3b. These measurements provide orientational constraints, in the form of θ_{CH}^{RFF} values for each of the four orientations of the $C_\alpha H_\alpha$ bond vectors for each of the asymmetric units in the unit cell. Since the LGCP method by itself does not resolve ϕ_{CH}^{RFF}, it is possible to consider this system to be analogous to a uniaxially aligned sample with numerous orientational species possessing the same chemical shift. Such a measurement by itself could provide a useful orientational constraint in a structure determining calculation of a uniaxially aligned biological macromolecule.

One limitation of this experiment that deserves attention is the existence of four degenerate solutions to Eq. (1) for any measured coupling value. Due to the $\sin 2\theta_{ij}^{RFF}$ dependence of δ and the inability to determine the absolute sign of the coupling frequency, the four orientations θ, $\frac{\pi}{2}+\theta$, $\frac{\pi}{2}-\theta$, and $\pi-\theta$ give the same coupling value. As such, the four values selected for Table 1 were selected of the four degeneracies that most closely matched those measured by X-ray indexing, and predicted by literature X-ray neutron diffraction structures. This degeneracy is removed in the 3D experiment.

3.3. Correlated dipolar measurements: orientation determination

To determine the orientation of the $C_\alpha H_\alpha$ bond vector it was necessary to relate the four θ_{CH}^{RFF} values with a neighboring vector whose orientation could separately be determined. For this purpose the LGCP experiment is supplemented with a series of five 2D rotor synchronized REDOR experiments that completely determine C–N vectors and the orientation of the crystal relative to the rotor. This approach takes advantage of the fact that the REDOR experiment, which is more suited to the lower frequency dipolar coupling frequencies of $^{13}C^{15}N$ pairs (unlike the LGCP experiment), is dependent on the azimuthal angle of the dipolar coupling vector in the rotor fixed frame.

The spectral splitting in the REDOR experiment can be related to the geometric factors of interest.

$$\omega_D = \omega_D\left(\theta_{CN}^{RFF}, \phi_{CN}^{RFF}\right) = \frac{\cos((\pi/2)\varphi)}{1-\varphi^2} 4\sqrt{2} D \sin\theta_{CN}^{RFF} \cos\theta_{CN}^{RFF} \sin\phi_{CN}^{RFF} \quad (5)$$

We include the previously derived term $\cos((\pi/2)\varphi)/(1-\varphi^2)$ that corrects for long dipolar recoupling pulse widths at high sample spinning speeds, where $\varphi = 2\tau_p/\tau_r$, τ_p is the π-pulse duration and τ_r is the rotor period [22]. Since there are four orientations present in the unit cell (defined by the $P_{2_12_12_1}$ symmetry), it is preferable to describe the data in a frame of reference defined by the crystallographic axes (i.e. crystal fixed frame—CFF). This simplifies the data analysis by relating the four orientational moieties by symmetry operators,

$$S_1 = \begin{pmatrix} 1 & 0 & 0 \\ 0 & 1 & 0 \\ 0 & 0 & 1 \end{pmatrix}, \quad S_2 = \begin{pmatrix} -1 & 0 & 0 \\ 0 & -1 & 0 \\ 0 & 0 & 1 \end{pmatrix}, \quad S_3 = \begin{pmatrix} -1 & 0 & 0 \\ 0 & 1 & 0 \\ 0 & 0 & -1 \end{pmatrix}, \quad S_4 = \begin{pmatrix} 1 & 0 & 0 \\ 0 & -1 & 0 \\ 0 & 0 & -1 \end{pmatrix} \quad (6)$$

and a frame transformation operator $\tilde{R}$.

The 2D REDOR data were simulated using a model based on Eq. (5), where the absolute orientation of the $C_\alpha N$ vectors in the RFF were substituted with the appropriate function of the CFF coordinates, the four symmetry operators S_k, and the three Euler angles of the CFF to RFF frame transformation operator $\tilde{R}(\alpha, \beta, \gamma)$ [13].

$$\begin{pmatrix} \sin\theta_{CN\ k}^{RFF}\cos\phi_{CN\ k}^{RFF} \\ \sin\theta_{CN\ k}^{RFF}\sin\phi_{CN\ k}^{RFF} \\ \cos\theta_{CN\ k}^{RFF} \end{pmatrix} = \tilde{R}(\alpha,\beta,\gamma) S_k \begin{pmatrix} \sin\theta_{CN}^{CFF}\cos\phi_{CN}^{CFF} \\ \sin\theta_{CN}^{CFF}\sin\phi_{CN}^{CFF} \\ \cos\theta_{CN}^{CFF} \end{pmatrix} \quad (7)$$

Eq. (7) displays the four sets of RFF coordinates can be expressed by one set of CFF coordinates and the three Euler angles. The five REDOR spectra collected from various initial azimuthal orientations (which relate to the γ Euler angle) shown in Fig. 4, provide enough data to reliably determine all five variables (Euler angles) defining the $C_\alpha N$ CFF coordinates and the crystal orientation. The details of this type of analysis are further detailed in a separate publication [13].

Finally, in order to relate the $C_\alpha H_\alpha$ and $C_\alpha N$ vectors, a 3D correlated pulse sequence outlined in Fig. 2b was applied to the single crystal L-alanine sample. The dipolar 2D plane from the 3D LGCP–REDOR experiment, taken at the C_α chemical shift, is shown in Fig. 5. We focus on and expand the region of the $^{13}C_\alpha{}^1H_\alpha$–$^{13}C_\alpha{}^{15}N$ correlated frequencies. Other spectral regions can be discarded, include the area near the center zero line ($|\omega_d| < 100$ Hz for the REDOR spectrum, $|\omega_d| < 3000$ kHz for the LGCP spectrum) and those much larger than $|\omega_d|$. The REDOR spectral center value is dependent on any offsets in the time domain, but since we utilized a shift of the baseline in the other indirect dimension (t_1, LGCP), the REDOR dimension is neither resolved nor reliable near zero frequency. In addition, we are unable to resolve the LGCP dimension near zero frequency, just as we were for 2D LGCP experiments. Thus there are effectively bleached regions of this spectrum. We illustrate one of the four identical regions of the dipolar correlation spectra (where the fourfold replication of the data resulted from a two dimensional Fourier transform applied to real data in both dimensions). Clearly the four $^1C_\alpha H_\alpha$–$C_\alpha N$ bond pairs' orientations can be resolved in this spectrum. Recording the dipolar splittings in a correlated fashion not only increased the resolution of each dipolar measurement, but more importantly allowed us to remove ambiguities in the interpretation. By correlating the REDOR splittings to the LGCP

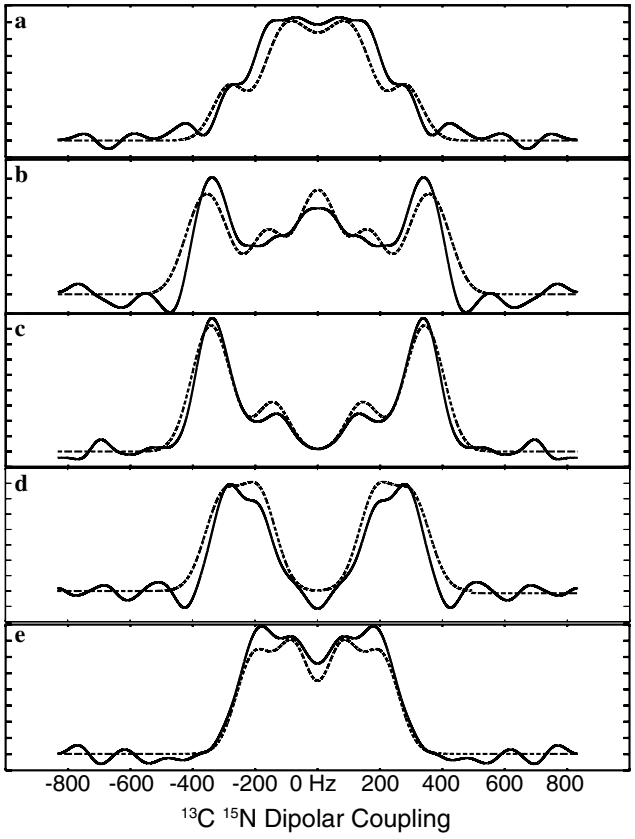

Fig. 4. $^{13}C^{15}N$ REDOR dipolar spectra of the alpha carbon of single crystal L-alanine (solid line). These spectra were recorded at incremental initial azimuthal angles (γ) of the rotor, controlled by the delay (τ_d) between the rotational synchronizing trigger and the ^1H channel $\pi/2$ pulse. For (a) $\tau_d = 0$ μs, (b) $\tau_d = 10$ μs, (c) $\tau_d = 20$ μs, (d) $\tau_d = 30$ μs, (e) $\tau_d = 40$ μs, with a sample spinning speed of $10{,}000 \pm 5$ Hz. The spectra were simultaneously simulated (dotted line) to an expression based on Eqs. (5) and (6) where the unknowns are the three Euler angles of the CFF to RFF frame transformation operator $\tilde{R}(\alpha, \beta, \gamma)$, and the polar and azimuthal angles of the CN vector in the crystal frame to find the best fit values of α, β, γ_0, θ_{CN}^{CFF},ϕ_{CN}^{CFF}.

splittings, the RFF polar angle θ_{CH}^{RFF} for all $C_\alpha H_\alpha$ bonds were associated with a particular symmetry operator S_k, as determined by the 2D REDOR experiment. The $C_\alpha H_\alpha$ coordinate vector can be expressed in spherical polar notation

$$\begin{pmatrix} \sin\theta_{CH\ k}^{RFF}\cos\phi_{CH\ k}^{RFF} \\ \sin\theta_{CH\ k}^{RFF}\sin\phi_{CH\ k}^{RFF} \\ \cos\theta_{CH\ k}^{RFF} \end{pmatrix} = \tilde{R}(\alpha,\beta,\gamma)S_k \begin{pmatrix} \sin\theta_{CH}^{CFF}\cos\phi_{CH}^{CFF} \\ \sin\theta_{CH}^{CFF}\sin\phi_{CH}^{CFF} \\ \cos\theta_{CH}^{CFF} \end{pmatrix} \tag{8}$$

making it is possible to equate the $C_\alpha H_\alpha \cos\theta_{CH\ k}^{RFF}$ to a function of the values of (θ_{CH}^{CFF},ϕ_{CH}^{CFF}), the Euler angles α and β (also determined by the REDOR experiments), and S_k. As there are four sets of equations (Equation 8 with $k = 1$–4) being fit to only two variables (θ_{CH}^{CFF},ϕ_{CH}^{CFF}) the solution is over determined and can be fit by RMS minimization. Table 1 shows that the results of this analysis are

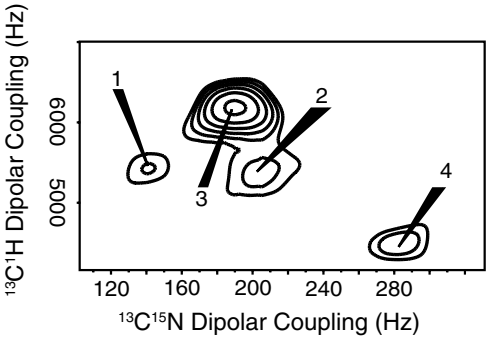

Fig. 5. The 2D $^{13}C^1H$ $^{13}C^{15}N$ dipolar correlation spectrum from a 3D LGCP–REDOR experiment on an L-alanine sample. The peaks represent correlations between $C_\alpha H_\alpha$ and $C_\alpha N$ splittings. One peak is present for each asymmetric unit in the unit cell, and each is labeled with the appropriate symmetry operator number (k) as defined in Eq. (6). The associated dipolar coupling values (ω_D^{CN}, ω_D^{CH}) given in Hz are (140, 5357), (205, 5301), (190, 6138), (283, 4436) for $k = 1$ through 4, respectively. This correlation and subsequent assignment of a symmetry operator to each $C_\alpha H_\alpha$ polar orientation (in the RFF) allows for global curve fitting routines described below allowed us to determine the orientation of the internuclear vectors relative to the crystal frame.

within excellent agreement with the X-ray and Neutron diffraction structures from the literature.

The dipolar spectra exhibit somewhat broad peak widths (300–500 Hz fwhm) principally due to a short value for $T_{1\rho}$ for the protons for this sample. The resulting precision in the determination of the frequency for spectra with favorable signal-to-noise rations is approximately 50 Hz. The B1 homogeneity in the active volume of the probe used for the measurement, and pulse missets can also have important effects on the peak widths and systematic errors, and therefore there is the possibility that other pulse sequences that are better compensated for inhomogeneity [23] could offer more precise determination of the dipolar frequency for favorable samples. In practice for these studies the signal-to-noise ratio was a more important factor determining the ultimate precision for the dipolar frequencies, as mentioned below.

4. Conclusion

This study illustrates that 2D LGCP data can be used to measure the polar coordinate (θ_{CH}^{RFF}) describing the $C_\alpha H_\alpha$ bond orientations present in the single crystal L-alanine sample, relative to the rotor frame, and that this measurement could similarly be made in a uniaxially aligned sample. The 3D LGCP–REDOR experiment, correlating the dipolar frequencies of the $^{13}C_\alpha{}^{15}N$ and the $^{13}C_\alpha{}^1H_\alpha$ couplings, was successfully employed to determine the complete $C_\alpha H_\alpha$ bond vector orientation in a single crystal. Along with the internuclear distance measured by the powder 2D LGCP experiment, this gives the absolute location of the $^1H_\alpha$ nucleus. The key to a reliable calculation of the total $C_\alpha H_\alpha$ geometry is being able to associate the $\theta_{CH_k}^{RFF}$ measurements of an orientational moiety, with the appropriate CFF based symmetry operator (S_k), as determined for the $C_\alpha N$ bond by 2D REDOR, and then use all four

orientations present in the unit cell to establish a complete solution. Such results are not readily available through any widely accessible method.

The work described herein also illustrates the ability to measure multiple orientations of $^{13}C^{1}H$ moieties sharing the same ^{13}C chemical shift in a uniaxially oriented sample, which could be a useful method of gathering orientational constraints for determining protein structures. Accurately confining the possible locations of hydrogen atoms in a protein has many potential applications, and there are few, readily accessible, alternative techniques. Development of such techniques will further distinguish SSNMR as a uniquely useful tool in protein structure determination.

References

[1] C.E. Kundrot, Which strategy for a protein crystallization project? Cellular and Molecular Life Sciences 61 (5) (2004) 525–536.

[2] T.I. Igumenova, A.E. McDermott, K.W. Zilm, R.W. Martin, E.K. Paulson, A.J. Wand, Assignments of carbon NMR resonances for microcrystalline ubiquitin, Journal Of The American Chemical Society 126 (21) (2004) 6720–6727.

[3] A. Bockmann, A. Lange, A. Galinier, S. Luca, N. Giraud, M. Juy, H. Heise, R. Montserret, F. Penin, M. Baldus, Solid state NMR sequential resonance assignments and conformational analysis of the 2×10.4 kDa dimeric form of the *Bacillus subtilis* protein Crh, Journal Of Biomolecular Nmr 27 (4) (2003) 323–339.

[4] J. Pauli, M. Baldus, B. van Rossum, H. de Groot, H. Oschkinat, Backbone and side-chain C-13 and N-15 signal assignments of the alpha-spectrin SH3 domain by magic angle spinning solid-state NMR at 17.6 tesla, Chembiochem 2 (4) (2001) 272–281.

[5] A.C. Zeri, M.F. Mesleh, A.A. Nevzorov, S.J. Opella, Structure of the coat protein in fd filamentous bacteriophage particles determined by solid-state NMR spectroscopy, Proceedings Of The National Academy Of Sciences Of The United States Of America (11) (2003) 6458–6463.

[6] F. Castellani, B. van Rossum, A. Diehl, M. Schubert, K. Rehbein, H. Oschkinat, Structure of a protein determined by solid-state magic-angle-spinning NMR spectroscopy, Nature 420 (6911) (2002) 98–102.

[7] T.A. Cross, J.R. Quine, Protein structure in anisotropic environments: development of orientational constraints, Concepts in Magnetic Resonance 12 (2) (2000) 55–70.

[8] J.R. Quine, T.A. Cross, Protein structure in anisotropic environments: unique structural fold from orientational constraints, Concepts in Magnetic Resonance 12 (2) (2000) 71–82.

[9] S.J. Opella, F.M. Marassi, Structure determination of membrane proteins by NMR spectroscopy, Chemical Reviews 104 (8) (2004) 3587–3606.

[10] D.A. Middleton, Z. Ahmed, C. Glaubitz, A. Watts, REDOR NMR on a hydrophobic peptide in oriented membranes, Journal of Magnetic Resonance 147 (2) (2000) 366–370.

[11] C. Glaubitz, A. Watts, Magic angle-oriented sample spinning (MAOSS): a new approach toward biomembrane studies, Journal of Magnetic Resonance 130 (2) (1998) 305–316.

[12] B.J. van Rossum, C.P. de Groot, V. Ladizhansky, S. Vega, H.J.M. de Groot, A method for measuring heteronuclear (H-1-C-13) distances in high speed MAS NMR, Journal of the American Chemical Society 122 (14) (2000) 3465–3472.

[13] B.J. Gross, Three Dimensional Structure Determination for Single Crystal and Uniaxially Aligned Amino Acids by Magic Angle Spinning Solid-State NMR, Columbia University, New York, 2004.

[14] A.E. Bennett, C.M. Rienstra, M. Auger, K.V. Lakshmi, R.G. Griffin, Heteronuclear decoupling in rotating solids, Journal of Chemical Physics 103 (16) (1995) 6951–6958.

[15] C.P. Jaroniec, B.A. Tounge, C.M. Rienstra, J. Herzfeld, R.G. Griffin, Measurement of C-13-N-15 distances in uniformly C-13 labeled biomolecules: J-decoupled REDOR, Journal of the American Chemical Society 121 (43) (1999) 10237–10238.

[16] G.A. Morris, R. Freeman, Selective excitation in Fourier-transform nuclear magnetic-resonance, Journal of Magnetic Resonance 29 (3) (1978) 433–462.

[17] J.W. Eaton, GNU Octave http://www.octave.org, 2.1.50-11, University of Wisconsin, 1998.

[18] R. Destro, R.E. Marsh, R. Bianchi, A low-temperature (23-K) study of L-alanine, Journal of Physical Chemistry 92 (4) (1988) 966–973.

[19] M.S. Lehmann, T.F. Koetzle, W.C. Hamilton, Precision neutron-diffraction structure determination of protein and nucleic-acid components. 1. Crystal and molecular structure of amino-acid L-alanine, Journal of the American Chemical Society 94 (8) (1972) 2657–2660.

[20] D.A. Case, Calculations of NMR dipolar coupling strengths in model peptides, Journal of Biomolecular Nmr 15 (2) (1999) 95–102.

[21] Y. Ishii, T. Terao, S. Hayashi, Theory and simulation of vibrational effects on structural measurements by solid-state nuclear magnetic resonance, Journal of Chemical Physics 107 (8) (1997) 2760–2774.

[22] C.P. Jaroniec, B.A. Tounge, C.M. Rienstra, J. Herzfeld, R.G. Griffin, Recoupling of heteronuclear dipolar interactions with rotational-echo double-resonance at high magic-angle spinning frequencies, Journal of Magnetic Resonance (1) (2000) 132–139.

[23] Vega, Alexander Controlling the effects of pulse transients and RF homogeneity in phase-modulated multiple-pulse sequences for homonuclear decoupling in solid-state proton NMR, Journal of Magnetic Resonance 170 (2004) 22–41.